Supplementary Information

Polylactic acid nanocomposite films with spherical nanocelluloses as efficient nucleation agents: Effects on crystallization, mechanical and thermal properties

Fangfang Lu [a], Houyong Yu [a*], Chenfeng Yan [a], Juming Yao [a, b, *]

Abstract In this data article provides non-isothermal crystallization behavior and polarized optical microscopy (POM) of the pure PLA and nanocomposites.

Value of the data The non-isothermal crystallization behavior can be used to calculate the crystallinity index of the pure PLA and nanocompsites, and the POM can be used to observe the morphologies, dimensions and numbers of the spherulites of the pure PLA and nanocompsites, which can provide a further insight into the crystallization behavior of pure PLA and nanocompsites.

Experimental Design, Materials and Methods

Non-isothermal crystallization and melting behavior

A TA instruments Q20 differential scanning calorimeter (DSC) measurements were performed in the temperature range from room temperature to 200 °C, at 2, 5, 10 and 20 °C min^{-1}, performing two heating and one cooling scans. Melting and cold crystallization temperatures and enthalpies (T_m, T_{cc} and ΔH_m, ΔH_{cc}) were determined from the second heating scan and glass transition temperature (T_g) were also measured. The degree of crystallinity (X_c) was calculated through Eq. (1).

$$X_c = 100\% \times [\frac{\Delta H_m - \Delta H_{cc}}{\Delta H_m^c}] \times \frac{1}{W_{PLA}} \quad (1)$$

where ΔH_m is the melting enthalpy, ΔH_{cc} is the cold crystallization enthalpy, ΔH_m^c is the melting heat associated to pure crystalline PLA (93 J g^{-1})[1] and W_{PLA} is the weight fraction of PLA in the nanocomposite.

[a]*The Key Laboratory of Advanced Textile Materials and Manufacturing Technology of Ministry of Education, College of Materials and Textile, Zhejiang Sci-Tech University, Hangzhou 310018, China. E-mail addresses:* phdyu@zstu.edu.cn.

[b]*National Engineering Lab for Textile Fiber Materials & Processing Technology, Zhejiang Sci-Tech University, Hangzhou 310018, China. E-mail addresses:* yaoj@zstu.edu.cn.

* Corresponding author. Fax: +86 571 86843619; Tel: +86 571 86843618.

Polarized optical microscopy (POM) was carried out on a Leitz Ortholux POL BKII optical microscope equipped with a Mettler Toledo Hot Stage FP82 controlled by Mettler FP90 Central Processor. Samples were prepared by melting sample between two cover slips on a hot plate and gently pressing them together with tweezers. Isothermal crystallization was recorded by heating the sample to 210 ^{o}C and holding for 5 min, then quenching (20 ^{o}C min^{-1}) to 110 ^{o}C.

Water absorption

The water absorption for pure PLA and the nanocomposite films were determined by previous reported method[2]. The samples were thin rectangular strips with an area of 10 cm^2, which were dried in a desiccator at 0% RH for 1 week until a constant weight was attained. Then the films were placed in a beaker at 100% RH and allowed to absorb water until a constant weight was reached. Water uptake was calculated as follows:

$$\text{water uptake} = \frac{w_t - w_0}{w_0} \times 100 \quad (1)$$

where W_0 and W_t are the weights of the sample before exposure to 100 % RH and after t hours of exposure to 100 % RH, respectively. Average values for five replicates were reported.

Water vapor permeability (WVP)

Water vapor permeability (WVP, in kg m m^{-2} s^{-1} Pa^{-1}) was determined according to previous reported methods[2-4]. Briefly, a 10 cm^2 sample was sealed in a bottle mouth and then into an ES-315 portable autoclave sterilizer at 120 ^{o}C for 10 min with a pressure of 110 kPa. When the temperature was cooled to room temperature, the penetration of water vapor through the film was almost finished, and the condensation water inside bottle was weighed. Finally, the WVP can be calculated as follows:

$$\text{WVP} = \frac{\Delta m}{t \times S \times P} \times e \quad (2)$$

where Δm is the mass change of the samples (kg) at time t (s), S is the test area (m^2), e is the film thickness (m), and P is the saturation pressure (Pa).

Overall migration tests

Overall migration tests were performed in two liquid food simulants (isooctane and 10% (v/v) ethanol) according to the Commission Regulation EU no. 10/2011 as previously reported[2,4-6]. Nanocomposite films with a total area of 10 cm^2 were immersed in a glass tube with 10 mL of each food simulant. Then the tube was completely sealed to avoid loss of the simulants. Samples in 10 % ethanol were kept in a controlled chamber at 40 ^{o}C for 10 days according to the Regulation EU no. 10/2011 (Commission Regulation EU 10/2011), while samples in isooctane were kept at 20 ^{o}C for 2 days according to the EN 1186-1:2002 (European Standard EN

1186-1:2002). When the incubation period was finished, the films were removed, the simulants were evaporated and the residue was weighed using an analytical balance with 0.1 mg precision. Then overall migration of simulants was taken as the weight ratio of residue per total simulant. For each sample, three replicates were performed and the average values were reported.

Data

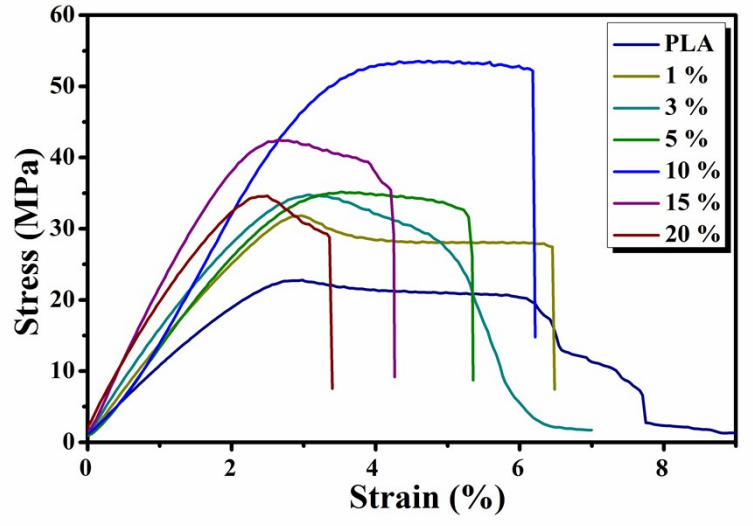

Figure S1 Representative stress-strain curves for pure PLA and the PLA/SCNF nanocomposite (selecting one experimental result).

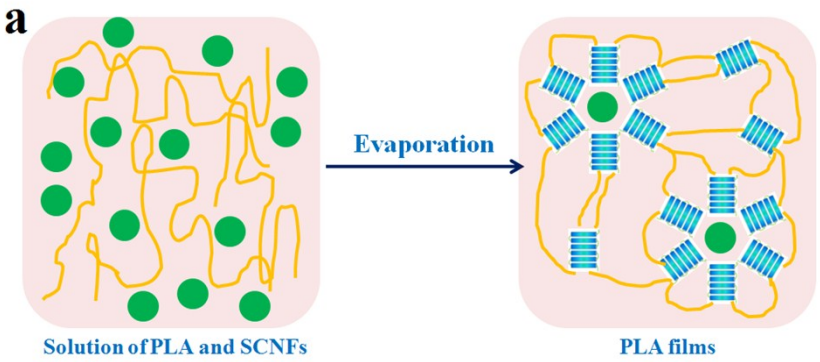

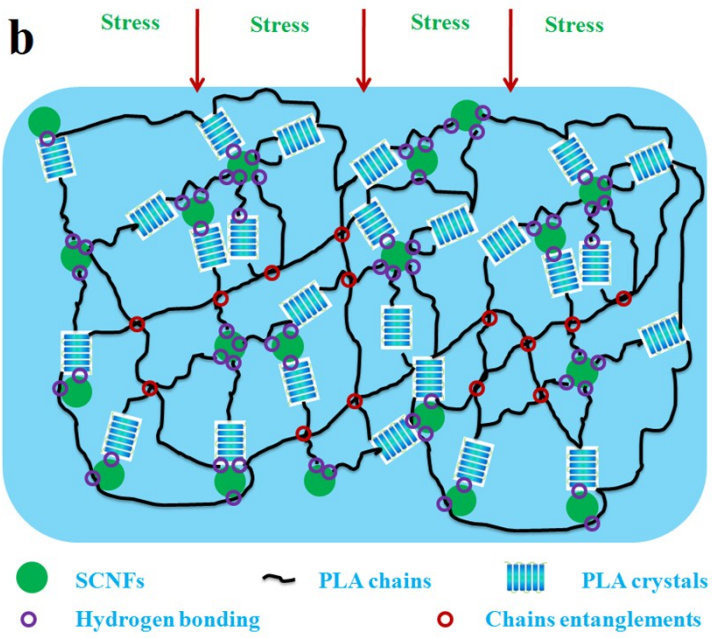

Figure S2 Possible schema of (a) the nucleation effect of SCNFs within the matrix, and (b) the the applied stress upon the PLA transferred by the more PLA crystals, hydrogen bonding interaction (or networks) or chain entanglements of PLA.

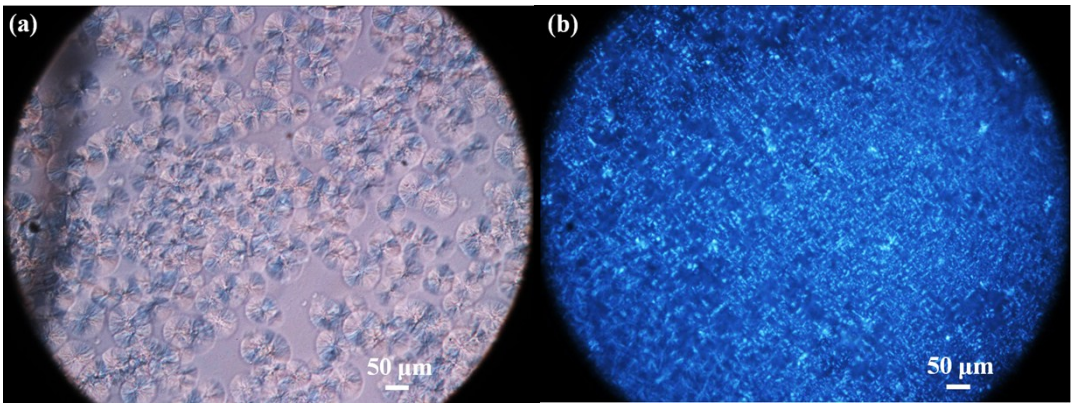

Figure S3 Polarized optical microscope (POM) images of (a) pure PLA, and (b) PLA/SCNF nanocomposites with 10 wt% SCNFs acquired after 10 min at 125 °C after quenched from melt at 210 °C.

Water uptake, water vapour permeability and overall migration

Generally, the increased crystallinity can improve not only tensile strength and modulus of the nanocomposites, but also the barrier and migration properties. Therefore, the water uptake and water vapour permeability (WVP) of the samples are shown in Figure S4(a). The pure PLA showed a water uptake of more than 6 % after being immersed in water for enough time, indicating its low resistance against water. In contrast, incorporation of SCNFs further improved the resistance against water of the nanocomposites. This phenomenon can be ascribed to the improved crystallinity and interfacial interaction between the PLA and SCNFs, which

strongly restricts the motions of the polymeric chains in water and increases the tortuosity in the nanocomposite films. Especially, the nanocomposites with 10 wt % SCNFs showed 78 % reduction in the water uptake compared to pure PLA. However, a negligible increase was observed up to 15 wt % and 20 wt % SCNFs (Figure S4(a)), which might be attributed to the reduction in the aggregated SCNFs/matrix interfacial area and decreased tortuosity in the nanocomposite films. Moreover, an obvious reduction in the WVP of the nanocomposite films was obtained by adding the SCNFs (Figure S4(a)). The WVP of the nanocomposites with 10 wt % SCNFs was reduced by 76 %, in comparison with pure PLA.

Results of overall migration for PLA based nanocomposites in both food simulants (i.e. isooctane and ethanol 10 %, v/v) are shown in Figure S4(b). All samples have the migration level in range from 30 to 160 µg kg^{-1}, which are all well below the legal overall migration limit (60 mg $kg^{-1}$of simulant) (Commission Regulation EU 10/2011). Moreover, SCNFs with increasing contents significantly decreased the migration level of stimulants, and the lowest migration level was achieved for the nanocomposite with 10 wt % SCNFs. This result was attributed to good interfacial adhesion or interaction between SCNFs and polymer matrix, and the increased crystallinity (due to good crystallization ability of the PLA brought by the nucleating effect of SCNFs), as previously discussed. It is interesting to highlight that the overall migration of pure PLA in ethanol 10 % v/v was higher than that in isooctane. This behavior can be explained by the fact that the hydrolysis of PLA and the formation of low molecular weight oligomers were more prone to migrate[7]. However, the nanocomposites showed high overall migration in isooctane. This is probably due to the increase in the polymer swelling caused by the isooctane which diminished the resistance to the release of additives to the medium by increasing the free volume in the polymer matrix[8].

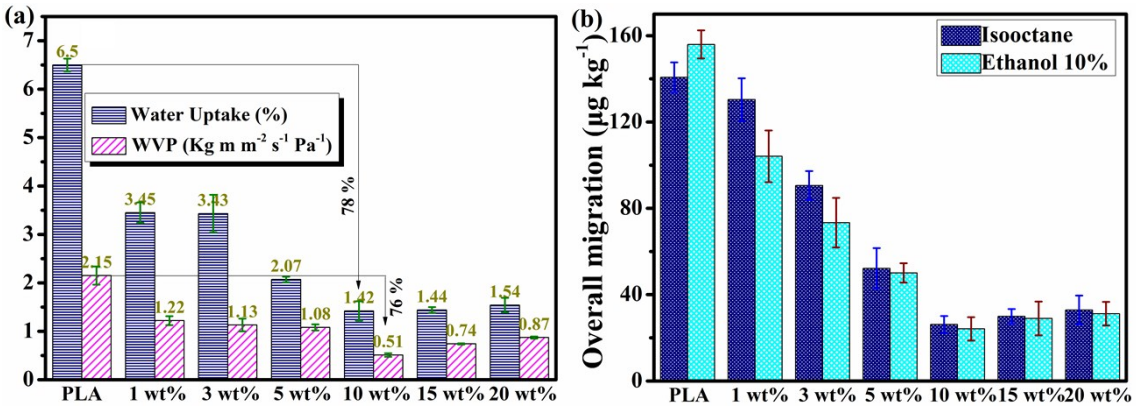

Figure S4. Water uptake and water vapour permeability (WVP) (a), and overall migration data in ethanol 10 % (v/v) and isooctane (b) as a function of SCNF contents for pure PLA and the nanocomposites.

Table S1 Thermal properties of PLA and PLA nanocomposites at the second heating scan.

Samples	Rate ($^oC\ min^{-1}$)	T_g (^oC)	ΔH_m ($J\ g^{-1}$)	T_{m1} (^oC)	T_{m2} (^oC)	H_{cc} ($J\ g^{-1}$)	T_{cc} (^oC)	X_c (%)
PLA	2	54.7	26.5	145.5	152.8	23.7	107.9	3.0
	5	57.1	23.4	147.5	152.2	20.9	120.4	2.6
	10	57.5	2.6	148.7	/	1.8	124.7	0.9
	20	60.9	0.5	150.3	/	0.1	129.0	0.4
1 %	2	56.2	29.6	146.5	153.8	21.1	107.2	9.2
	5	57.8	23.7	148.5	153.2	18.3	119.6	5.9
	10	58.5	4.7	149.9	/	4.1	124.5	0.6
	20	61.7	0.5	150.6	/	0.1	129.4	0.5
3 %	2	59.6	38.8	148.2	155.1	25.0	106.2	13.9
	5	59.3	18.0	150.2	153.6	9.2	119.6	9.0
	10	60.9	3.5	151.4	/	2.5	123.5	1.2
	20	62.4	0.6	152.5	/	0.1	127.4	0.6
5 %	2	60.6	34.6	148.4	155.5	19.3	105.2	17.3
	5	62.0	17.2	151.2	154.9	8.4	118.8	9.7
	10	62.4	3.0	152.9	/	1.4	122.5	1.8
	20	63.6	/	/	/	0.1	126.2	/
10 %	2	59.1	34.3	150.6	156.5	17.7	104.3	19.8
	5	62.2	12.6	151.7	154.6	3.8	117.9	10.5
	10	63.2	4.2	154.1	/	1.2	121.7	3.6
	20	63.8	/	/	/	0.1	125.5	/
15 %	2	58.9	37.8	148.7	155.5	23.1	107.7	18.6
	5	61.2	16.8	150.5	154.4	9.2	119.8	9.6
	10	61.9	4.7	151.9	/	2.7	125.2	3.0
	20	63.8	0.6	152.5	/	0.1	130.6	0.8
20 %	2	58.9	42.7	148.2	155.1	32.1	112.4	14.2
	5	60.0	19.0	149.7	153.9	11.8	123.2	9.7

	10	60.7	2.5	150.5	/	0.6	126.4	2.6
	20	63.1	0.1	152.0	/	0.1	12	0.1

References

1 M. P. Arrieta, E. Fortunati, F. Dominici, J. López and J. M. Kenny, *Carbohydrate Polymer*, 2015, **121**, 265-275.

2 H. Y. Yu, Z. Y. Qin, B. Sun, X. G. Yang and J. M. Yao, *Compos Sci Technol*, 2014, **94**, 96-104.

3 S. K. Pankaj, C. N. Bueno-Ferrer, N. Misra, L. O'Neill, A. Jiménez, P. Bourkea and P.J. Cullena, *Innov Food Sci Emerg*, 2014, **21**, 107-113.

4 E. Fortunati, M. Peltzer, I. Armentano, L. Torre, A. Jiménez and J. M. Kenny, *Carbohydr Polym*, 2012, **90**, 948-956.

5 E. Fortunati, F. Luzi, D. Puglia, R. Petrucci, J. M. Kenny and L. Torre, *Ind Crop Prod*, 2015, **67**, 439-447.

6 E. Fortunati, D. Puglia, F. Luzi, C. Santulli, J. M. Kenny and L. Torre, *Carbohydr Polym*, 2013, **97**, 825-836.

7 E. Fortunatia, S. Rinaldi, M. Peltzer, N. Bloise, L. Visai, I. Armentano, A. Jiménez, L. Latterini and J. M. Kenny, *Carbohydr Polym*, 2014, **101**, 1122-1133.

8 J. Alin and M. Hakkarainen, *J Agr Food Chem*, 2011, **59**, 5418-5427.